Spatiotemporal beam-plasma instabilities in the ultrarelativistic regime

Yuliia Mankovska[1] on behalf of the E305 collaboration[1-9]

[1] LOA, Palaiseau, France, [2] University of Oslo, Norway, [3] CU Boulder, USA, [4] SLAC, Menlo Park, USA, [5] CEA DAM, Arpajon, France, [6] UCLA, Los Angeles, USA, [7] MPIK, Heidelberg, Germany, [8] IST, Lisbon, Portugal, [9] Stony Brook, New York, USA

Theoretical study of relativistic beam-plasma systems

Instability growth

The E305 experiment at FACET-II facility at SLAC is dedicated to study the relativistic kinetic beam-plasma instabilities, including spatiotemporal dynamics, interplay of different modes, nonlinear stage etc.

Previously performed theoretical study shows that for the beam-plasma systems with parameters relevant to the E305 experiment the prevailing instability is the oblique two-stream instability (OTSI) and its growth has spatiotemporal character (Fig.1, 2).

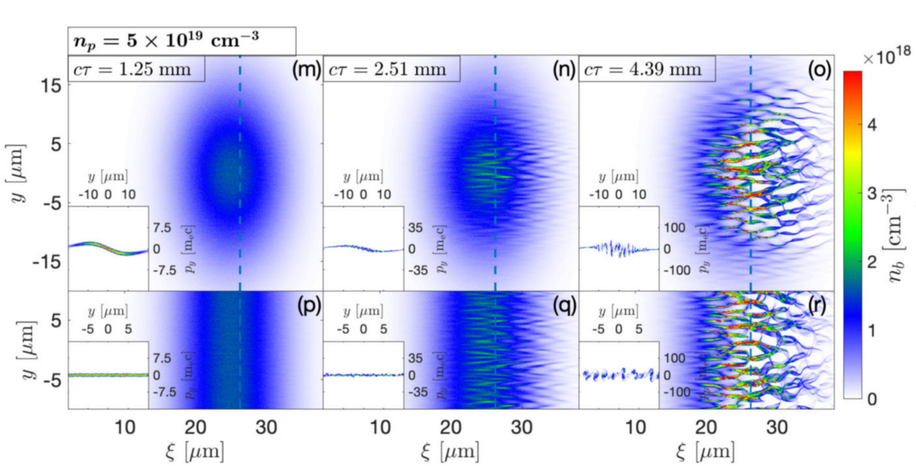

Fig. 1: Simulated electron-beam-density maps at different propagation distances (increasing from left to right) in a uniform plasma. In the top row (m)-(o) the transverse beam profile is Gaussian with $\sigma_r = 10\mu m$, the bottom row (p)-(r) corresponds to the transversely infinite beam.

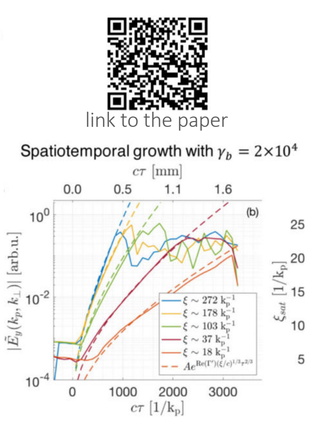

Fig. 2: Electric field amplitude evolution for different beam slices ξ (solid lines) compared to the spatiotemporal model $Ae^{\mathbb{R}e(\Gamma')(\xi/c)^{1/3}\tau^{2/3}}$ (dashed lines).

Instability saturation

To study the behaviour of saturation of relativistic kinetic plasma instabilities 2D PIC simulations have been performed. They show that the rear of the beam reaches the saturation faster than the beam front. The maximal value of the electric field amplitude also grows from front to rear (Fig. 3).

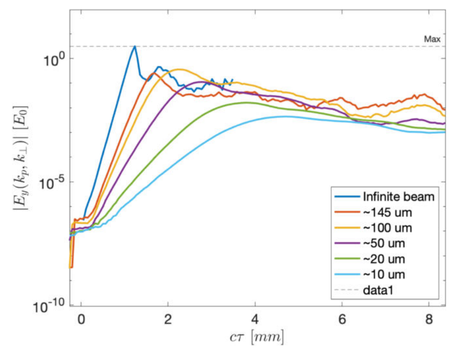

Fig. 3: Electric field amplitude evolution for different beam slices compared to the infinite beam evolution.

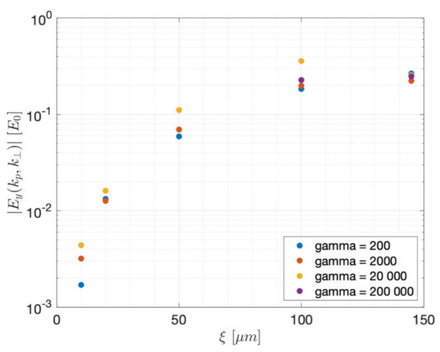

Fig. 4: Saturation values of the electric field amplitude depending on the position in the beam ξ for different beam energies γ_b (dots of different colours).

Systems with different beam energies have also been investigated. We can see (Fig. 4), that the spatiotemporality of instability saturation preserves regardless the beam energy, and studied cases show very similar maximal values of saturation.

Experimental detection of the instability

Dark-field shadowgraphy

The goal of this method is to image the signature that filamented beam in plasma leaves behind.

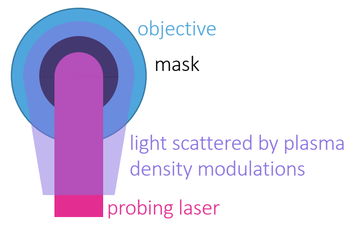

Fig. 5: A simplified scheme of the dark-field shadowgraphy.

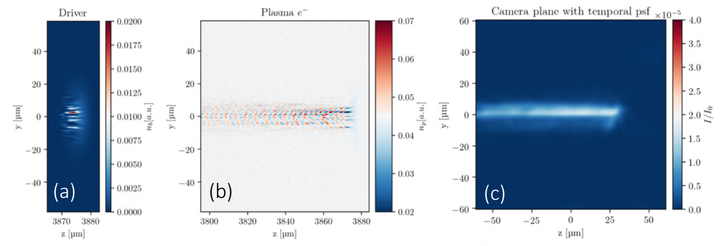

Fig. 6: Simulation of the dark-field shadowgraphy. The example of the signal on camera (c) that can be obtained with this diagnostic.

The electron beam propagates through plasma, provided by the gas jet. Then the probe laser goes through the plasma modulated by the beam. The objective is installed after the interaction point and the blocking screen slightly bigger than the probe laser radius is attached to it. This provides the possibility to capture not the initial probe, but only the light, scattered by plasma density modulations (Fig. 5, 6).

Chirped beam

This experimental detection technique relies on the use of ultrahigh-quality chirped beams with a correlation between the particle energy and its longitudinal position. If after propagation through plasma such beam is deflected by the magnetic field onto a scintillating screen, the spatiotemporality of the instability would be manifested in the correlation between the coordinate on the screen with the transverse momentum spread (Fig. 7).

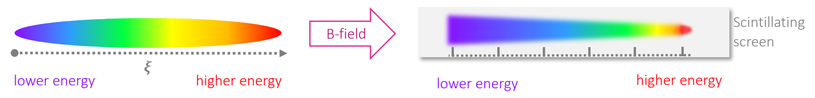

Fig. 7: A simplified scheme of the chirped beam use.

Instability seeding

The E336 experiment at the FACET-II facility at SLAC is devoted to the interaction of the particle beams with special nanostructured targets. As the beam would propagate through it, the nanotubes would force the transverse modulation onto the beam, seeding the instability (Fig. 8).

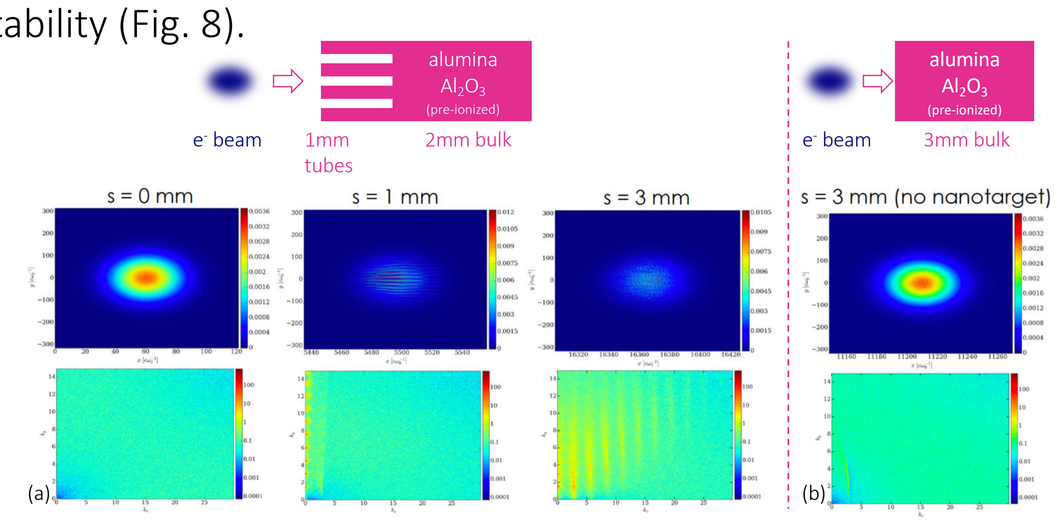

Fig. 8: The example of the beam interaction with the nanostructured target (a) and the comparison to the beam interaction with the analogous bulk target (b).

Acknowledgements

Full list of E305 collaborators: E. Adli[2], I. Andriyash[1], R. Ariniello[3,4], J. Cary[3], S. Corde[1], X. Davoine[5], C. Doss[3], H. Ekerfelt[4] , C. Emma[4], J. Faure[5], F. Fiuza[4], E. Gerstmayr[4], S. Gessner[4], M. F. Gilljohann[1], L. Gremillet[5], M. Hogan[4], K. Hunt-Stone[3], C. Joshi[6], C. Keitel[7], A. Knetsch[1,4], O. Kononenko[1], V. Lee[3], M. Litos[3], A. Marinelli[4], K. Marsh[6], A. Matheron[1], S. Montefiori[7], W. Mori[6], N. Nambu[6], Z. Nie[6], B. O'Shea[4], S. Passalidis[5], J. Peterson[4], A. Sampath[7], P. San Miguel Claveria[1,8], D. Storey[4], M. Tamburini[7], N. Vafaei-Najafabadi[9], Y. Wu[6], X. Xu[6], V. Yakimenko[4], J. Yan[9], V. Zakharova[1], C. Zhang[6].

This poster presentation has received support from the European Union's Horizon 2020 Research and Innovation programme under Grant Agreement No 101004730.